Journal of Civil Engineering and Architecture 14 (2020) 516-524
doi: 10.17265/1934-7359/2020.09.006

Effect of Lateral Restraint on Buckling Behaviour of a Thin-Walled Z-Section Column

Tanja Mališ[1], Diana Šimić Penava[2] and Antonia Jaguljnjak Lazarević[1]

1. Faculty of Mining, Geology and Petroleum Engineering, University of Zagreb, Pierottijeva 6, Zagreb 10000, Croatia

2. Faculty of Civil Engineering, University of Zagreb, Fra Andrije Kačića-Miošića 26, Zagreb 10000, Croatia

Abstract: The aim of this paper is to interpret the effect of lateral restraint on buckling behaviour of a Z-cross section column subjected to pure axial load. Adequate analytical solutions are compared with the numerical and experimental results obtained for specimens both laterally free and those restrained by trapezoidal steel sheeting. Compared to the unrestrained column, a large relative increase of critical loads is detected. Therefore, further optimization of such structural elements is possible.

Key words: Z-section column, lateral restraint, buckling resistance, finite element method.

1. Introduction

Thin-walled open section columns and beams are very efficient and therefore interesting in structural design, but with behaviour more complicated than is generally the case for closed or solid cross-section elements [1, 2]. Because of their characteristic shape, formed of slender parts, tendency towards complicated loss of stability often arises. The form of stability loss may be flexural, torsional or a combination of both. More generally, lateral or local buckling is always possible. In the case of solid cross sections, the flexural modes are the most dominant [3, 4].

Existing researches mainly apply to the stability of thin-walled open cross section beams, where analyses are limited to beams subjected to gravity or lifting load defined by various standards [5-7]. On the contrary, behaviour of laterally restrained axially loaded column has not been the subject of systematic research, and satisfactory treatment by modern standards is missing [3, 8].

This research is focused on the case when a thin-walled Z-section column is centrally loaded. The unrestrained and various laterally restrained models are discussed. The effects of local buckling are avoided by selecting appropriate shapes and thicknesses of cross sections and edge fold stiffeners of the flanges. Therefore, only the overall buckling resistance is the subject of this research. The analytical results are compared with values obtained by the finite element method (FEM) [9], and additionally confirmed by carefully designed experiments.

2. General Analytical Solutions for Different Lateral Supports

Stability equations for the laterally free or restrained beams with the line connection (stiffener) parallel to the major centroidal axes of the cross-sectional inertia already exist in the literature [2]. Here, the equations for column with the line connection inclined at the arbitrary angle to the major centroidal axes are derived.

Four different cases are analysed: an unrestrained column, a column laterally restrained by either a horizontal or a vertical rigid connection (with respect to the cross-sectional plane) and a column laterally restrained by a horizontal rigid and rotational elastic connection (Fig. 1).

Corresponding author: Diana Šimić Penava, Ph.D., professor, research field: thin-walled structures.

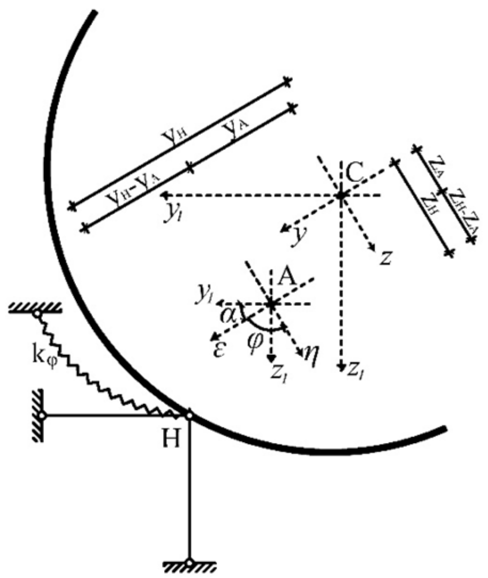

Fig. 1 Arbitrary cross section with lateral supports.

2.1 Laterally Unsupported Column

Equilibrium equations under centric load F in the moment of stability loss are [2, 8, 10]:

$$\begin{aligned} EI_y\eta^{\mathrm{IV}} + F\eta'' - y_A F\varphi'' &= 0 \\ EI_z\varepsilon^{\mathrm{IV}} + F\varepsilon'' + z_A F\varphi'' &= 0 \\ EI_\omega\varphi^{\mathrm{IV}} + (r^2F - GI_t)\varphi'' + z_A F\varepsilon'' - y_A F\eta'' &= 0 \end{aligned} \quad (1)$$

Points C and A are the section's centroid and the shear centre (SC) respectively (Fig. 1). y_A and z_A are the coordinates of SC. ε and η are the displacement components of SC in the direction of the major axes of inertia y and z, while φ is a rotation angle of the cross section around the SC vertical axis. E and G are the elasticity and the shear modulus, I_y, I_z and I_ω are the main axial and sectorial moments of inertia, while I_t is the torsional moment of inertia. Factor r^2 is

$$r^2 = \frac{I_y + I_z}{A_S} + y_A^2 + z_A^2 \quad (2)$$

with A_S as the area of the cross section. For the non-trivial solution, the determinant of the homogenous system of Eq. (1) must vanish:

$$\begin{vmatrix} F_z - F & 0 & -z_A \cdot F \\ 0 & F_y - F & y_A \cdot F \\ -z_A \cdot F & y_A \cdot F & r^2 \cdot (F_\omega - F) \end{vmatrix} = 0 \quad (3)$$

and characteristic equation has three real, distinct positive roots: F_1, F_2 and F_3 [2]. Here, F_y and F_z are the Euler critical loads that correspond to the pure flexural buckling:

$$F_y = \frac{\pi^2 EI_y}{l_i^2},\ F_z = \frac{\pi^2 EI_z}{l_i^2} \quad (4)$$

where the buckling length l_i depends on the boundary conditions. F_ω is the critical load for the torsional loss of stability:

$$F_\omega = \frac{1}{r^2} \cdot \left(\frac{\pi^2 EI_\omega}{l_i^2} + GI_t\right) \quad (5)$$

The most important buckling load of the column is:

$$F_{\mathrm{cr}} = F_{\min} = F_1 \quad (6)$$

If F_1 is less than F_y, F_z and F_ω, the loss of stability is flexural-torsional, if $F_1 = F_y$ or $F_1 = F_z$, pure flexural buckling appears, and if $F_1 = F_\omega$, pure torsional buckling occurs.

2.2 Column Laterally Supported by a Horizontal Rigid Connection

Coordinates of the lateral restraint point H are y_H and z_H (Fig. 1). Axis y_1 is parallel and z_1 is perpendicular to the lateral restraint, and α is the angle between the major axis of inertia y and axis y_1. Horizontal displacement of the point H is equal to zero. Using that condition, equilibrium equations are:

$$\begin{aligned} &E\left(I_y + tg^2\alpha I_z\right)\eta^{\mathrm{IV}} + F sec^2\alpha\,\eta'' + EI_z\,tg\alpha\,D_1\varphi^{\mathrm{IV}} \\ &\qquad + F(-y_A + z_H tg\alpha + \Delta y tg^2\alpha)\varphi'' \\ &\qquad = 0 \\ &EI_z\,tg\alpha\,D_1\eta^{\mathrm{IV}} + F(-y_A + z_H tg\alpha + \Delta y\,tg^2\alpha)\eta'' \\ &\qquad + EI_\omega\varphi^{\mathrm{IV}} + EI_z{D_1}^2\varphi^{\mathrm{IV}} + \\ &\begin{Bmatrix} F[(\Delta y\,tg\alpha + z_H)^2 - {z_A}^2 + r^2] - \\ GI_t \end{Bmatrix}\varphi'' = 0 \end{aligned} \quad (7)$$

where $\Delta y = y_H - y_A$, $\Delta z = z_H - z_A$, and $D_1 = \Delta z + \Delta y\,tg\alpha$. For the non-trivial solution, $\det \mathbf{B} = 0$, where

$$b_{1,1} = E\frac{\pi^2}{{l_i}^2}\left(I_y + tg^2\alpha I_z\right) - F sec^2\alpha$$

$$b_{1,2} = b_{2,1} = EI_z tg\alpha\frac{\pi^2}{{l_i}^2}D_1 +$$
$$F(y_A - z_H tg\alpha - tg^2\alpha\,\Delta y) \quad (8)$$

$$b_{2,2} = E\frac{\pi^2}{l_i^2}\left(I_\omega + I_z D_1^2\right) + \{GI_t - F[(\Delta y\, tg\alpha + z_H)^2 - z_A^2 + r^2]\}$$

are obtained for the clamped-sliding beam ($l_i = l_T = l$). Two real positive roots, F_1 and F_2 exist and the critical buckling load is also $F_{\min} = F_1$.

2.3 Column Laterally Supported by a Vertical Rigid Connection

Here, vertical displacement of the point *H* is equal to zero (Fig. 1). According to that restraint, equilibrium equations are:

$$E\left(I_z + tg^2\alpha I_y\right)\varepsilon^{\mathrm{IV}} + Fsec^2\alpha\, \varepsilon'' + EI_y tg\alpha D_2 \varphi^{\mathrm{IV}} + F(z_A + y_H tg\alpha - tg^2\alpha \Delta z)\varphi'' = 0$$

$$EI_y tg\alpha D_2 \varepsilon^{\mathrm{IV}} + F(z_A + y_H tg\alpha - \Delta z\, tg^2\alpha)\varepsilon'' + EI_\omega \varphi^{\mathrm{IV}} + EI_y D_2^2 \varphi^{\mathrm{IV}} + \{F[D_2(y_H - \Delta z\, tg\alpha) + y_A D_2 + r^2] - GI_t\}\varphi'' = 0 \quad (9)$$

where $D_2 = \Delta y - \Delta z\, tg\alpha$ and matrix **B** needed for the stability condition (with $F_1 < F_2$) is given by:

$$b_{1,1} = E\frac{\pi^2}{l_i^2}\left(I_z + tg^2\alpha I_y\right) - Fsec^2\alpha$$

$$b_{1,2} = b_{2,1} = EI_y tg\alpha \frac{\pi^2}{l_i^2} D_2 + F(-z_A - y_H tg\alpha + tg^2\alpha\, \Delta z) \quad (10)$$

$$b_{2,2} = E\frac{\pi^2}{l_i^2}\left(I_\omega + I_y D_2^2\right) + \{GI_t - F[D_2(y_H - \Delta z\, tg\alpha) + y_A D_2 + r^2]\}$$

2.4 Column Laterally Supported by a Horizontal Rigid and by a Rotational Elastic Connection

Horizontal displacement of the point *H* (Fig. 1) is equal to zero as in Section 2.2. Rotational elastic stiffness k_φ [moment/length/rad] is defined as a moment per unit length related to the unit rotation of infinitely close column cross-sections. Equilibrium equations are:

$$E\left(I_y + tg^2\alpha I_z\right)\eta^{IV} + Fsec^2\alpha\, \eta'' + EI_z\, tg\alpha\, D_1 \varphi^{IV} + F(-y_A + z_H tg\alpha + \Delta y tg^2\alpha)\varphi'' = 0$$

$$EI_z\, tg\alpha\, D_1 \eta^{IV} + F(-y_A + z_H tg\alpha + \Delta y\, tg^2\alpha)\eta'' + EI_\omega \varphi^{IV} + EI_z D_1^2 \varphi^{IV} + \{F[(\Delta y\, tg\alpha + z_H)^2 - z_A^2 + r^2] - GI_t\}\varphi'' + k_\varphi \varphi = 0 \quad (11)$$

As previously mentioned, coefficients needed for the solution are:

$$b_{1,1} = E\frac{\pi^4}{l_i^4}\left(I_y + tg^2\alpha I_z\right) - F\frac{\pi^2}{l_i^2} sec^2\alpha$$

$$b_{1,2} = b_{2,1} = EI_z tg\alpha \frac{\pi^4}{l_i^4} D_1 + F\frac{\pi^2}{l_i^2}(y_A - z_H tg\alpha - tg^2\alpha\, \Delta y) \quad (12)$$

$$b_{2,2} = E\frac{\pi^4}{l_i^4}\left(I_\omega + I_z D_1^2\right) + \frac{\pi^2}{l_i^2}\{GI_t - F[(\Delta y\, tg\alpha + z_H)^2 - z_A^2 + r^2]\} + k_\varphi$$

2.5 Application to a Z-Section Column

Calculation of critical loads for columns of 1.7 m high, with the Z-cross-section 80/40/20/3 is carried out (Fig. 2). Such models are specifically selected to expand previous research on the C-cross-section models [8].

The cross-sectional data are: A_S = 564 mm^2, I_y = 710,803.1 mm^4, I_z = 84,210.9 mm^4, I_t = 1,692 mm^4, I_ω = 278,492,097.5 mm^6, r^2 = 1,409.6 mm^2, y_A = 0 and z_A = 0. Mechanical properties of steel are determined by laboratory tests on five standard specimens according to EN ISO 6892-1 (Fig. 3a). After appropriate averaging, the mechanical properties are: *E* = 203.8 GPa, *G* = 79.3 GPa and the yield strength is σ_y = 306 MPa. In Fig. 3b the elastic part and the yield plateau of the idealised stress-stain curve are enlarged, and five regions of different tangent moduli are detected.

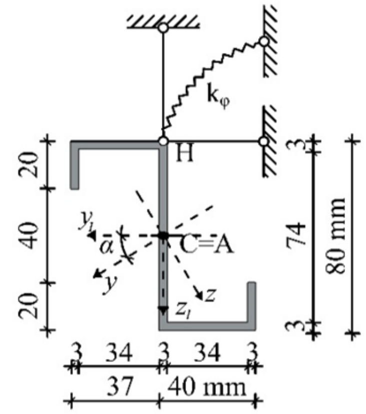

Fig. 2 Z-cross section.

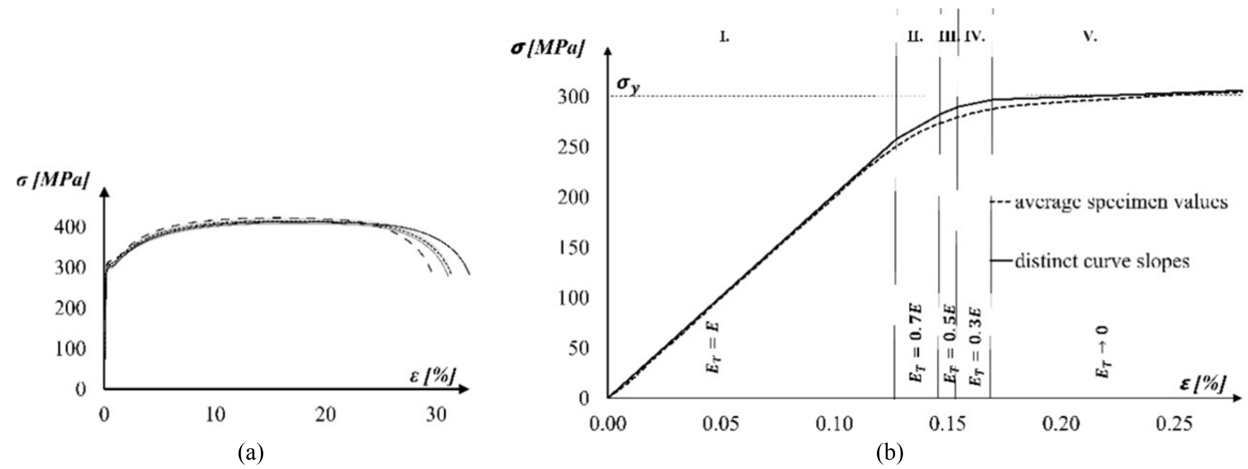

Fig. 3 (a) Stress-strain curves for 5 Z-specimens and (b) enlarged part of the idealised stress-strain curve.

Table 1 The analytical results for the Z-section column.

Section	$l_i = 2l$		$l_i = l$		$l_i = 0.7l$		$l_i = 0.5l$	
	F_{cr} [kN]	BT	F_{cr} [kN]	BT	F_{cr} [kN]	BT	F_{cr} [kN]	BT
2.1	14.6	F	58.4	F	119.1	F	159.6*	F
2.2	53.3	F + T	123.5	F + T	151.3*	F + T	163.6*	F + T
2.3	43.9	F + T	145.5*	F + T	163.6*	F + T	167.5*	T
2.4	90.3	F + T	146.0*	F + T	159.6*	F + T	163.6*	F + T

BT—buckling type, F—pure flexural, T—pure torsional, F + T—flexural-torsional.

Torsional stiffness, realised by adequately fastened sheeting, with ribs perpendicular to the column, is determined according to Eurocode 3 (EC3) [11]. Laboratory tests and the analytical solution are combined and the rotational stiffness $k_\varphi = 0.9$ kNm/m/rad is determined [8].

Critical forces $F_{cr} = F_1$ for the Z-column (α = 31.32°), for each of the four analytical cases and typical buckling lengths are shown in Table 1. Data marked with "*" are obtained using the tangent modulus concept (buckling above the proportional limit σ_P is detected), which gives results on the safe side [12, 13]. Depending on the stress level, value E_T according to the regions I to V (Fig. 3b) gives the correct critical forces. All calculations are made with the Wolfram Mathematica.

Highlighted cases were additionally analysed by experiments and the FEM, as will be discussed in the following sections.

3. Experimental and Numerical Determination of Critical Forces

Z-column clamped at the bottom, and with the sliding restraint at the top is analysed. Two different cases are considered: laterally unsupported and by trapezoidal steel sheeting T 40/245/1 mm restrained column (Fig. 4). According to the EC3 [11], the latter case can be properly modelled by the theoretical approach described in Section 2.4, providing adequate sheeting stiffness.

3.1 Experimental Models

Stability analysis of the unrestrained Z-cross section column and of the column laterally restrained by trapezoidal steel sheeting has been carried out experimentally using a hydraulic static press machine at the Department of Engineering Mechanics, Faculty of Civil Engineering, University of Zagreb, Croatia. At the column ends thick plates are welded. The bottom plate is properly fixed on the ground, and the top plate is sliding under another, mounted on the machine head (Fig. 5). Mechanical properties of plates and column are the same.

The columns were gradually loaded by force increment ΔF = 30 kN until the loss of stability occurred. Fig. 5a shows an unrestrained and Fig. 5b shows a laterally restrained column, both in the post buckling state. Inductive strain gauges measured the

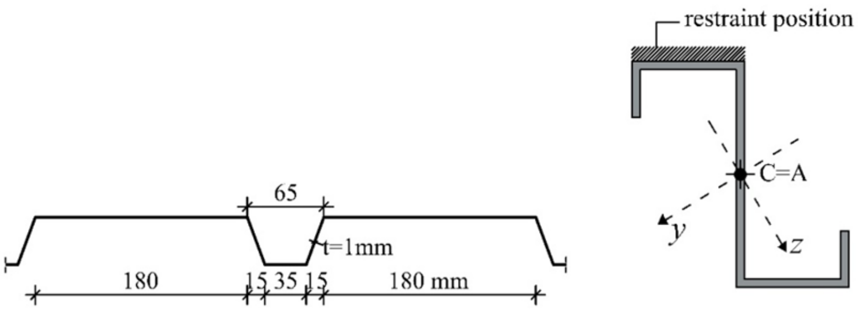

(a) (b)

Fig. 4 (a) Dimensions and (b) position of trapezoidal steel sheeting.

(a) (b)

Fig. 5 Loss of stability: (a) unrestrained, (b) laterally restrained column.

lateral displacement and the resistance strain gauges measured the longitudinal strain in the column. Fig. 6 shows resistance strain gauge positions (T1 to T6) at the mid-height section and the stress-strain diagrams for the longitudinal direction of the unrestrained and laterally restrained column. Fig. 7 shows the force-displacement diagram for lateral direction measured with the inductive strain gauges (I1 to I6) at the mid-height section of the unrestrained and laterally restrained column. Extension of the inductive strain gauges gives negative displacement and shrinkage gives positive displacement.

The loss of stability of the unrestrained column happened at the critical force $F_{\mathrm{cr}} = 60$ kN due to pure flexural in-plane buckling (Fig. 5a). The displacement increment after F_{cr} is not proportional to the force increment (when the model starts to lose stability). The model was loaded once again, but it could not withstand more than 63 kN (Fig. 7a), while the loss of stability occurred at the critical force of 60 kN.

The loss of stability of the laterally restrained column happened at $F_{\mathrm{cr}} = 150$ kN due to simultaneous twisting and lateral out-plane bending (Fig. 5b). After 150 kN the displacement and load increment are not proportional. The model was loaded once again, but it could not withstand a force greater than 150 kN (Fig. 7b).

3.2 Finite Element Models

Buckling analysis is carried out numerically, by using the FEM with the SAP2000 v21 software [14]. The thin-walled columns are modelled by shell elements, using the geometrical and mechanical properties from the experimental and analytical study.

For the unrestrained column linear elastic instability occurs at $F_{cr} = 58.5$ kN in flexural (pure) buckling mode (Fig. 8a). The laterally restrained column buckles at $F_{cr} = 145.5$ kN in nonlinear region and flexural-torsional buckling mode (Fig. 8b).

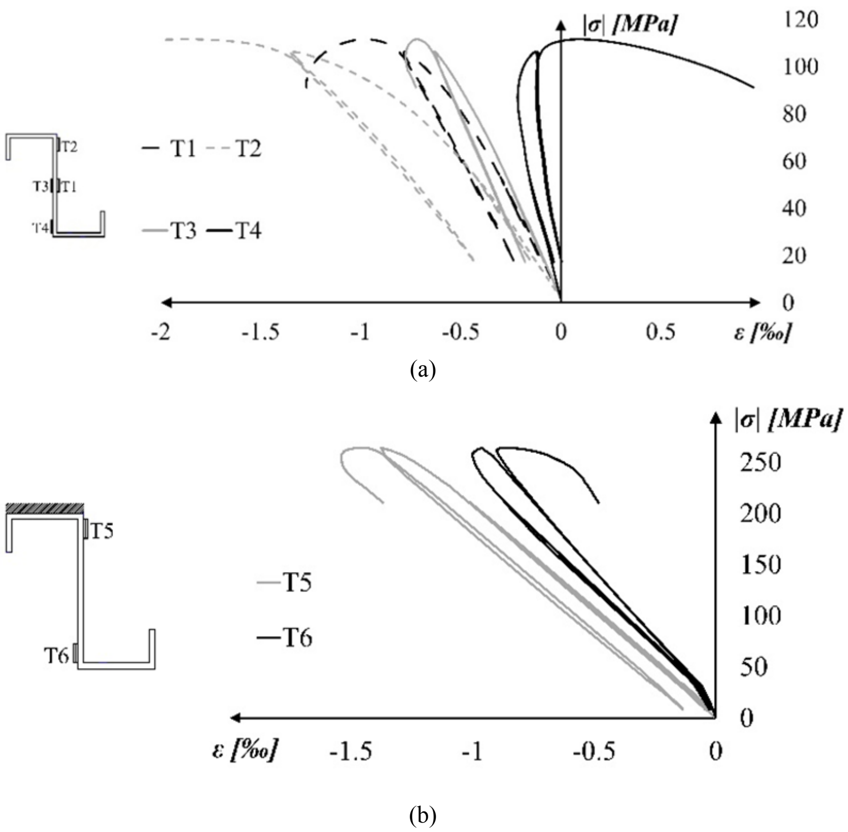

Fig. 6 Stress-strain diagram for the longitudinal direction: (a) unrestrained, (b) laterally restrained column.

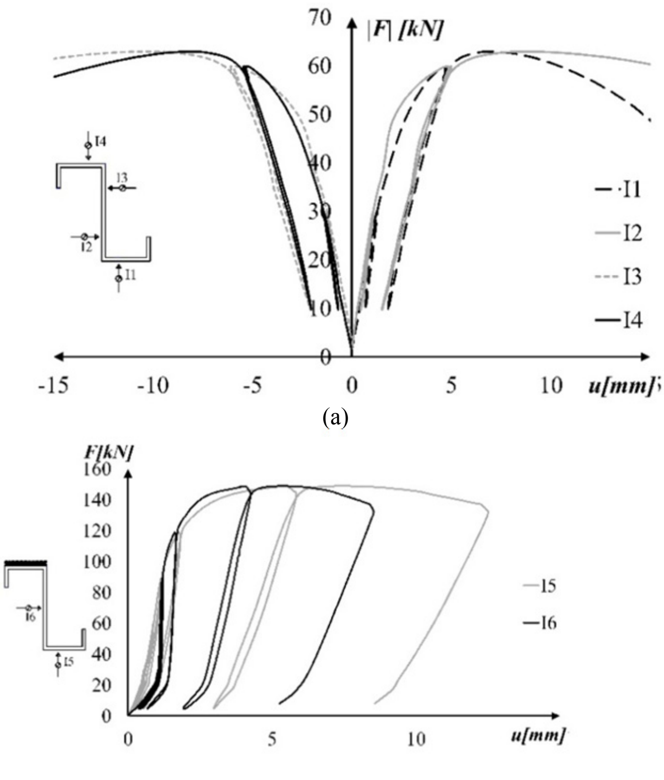

(a)

(b)

Fig. 7 Force-displacement diagram for lateral direction: (a) unrestrained, (b) laterally restrained column.

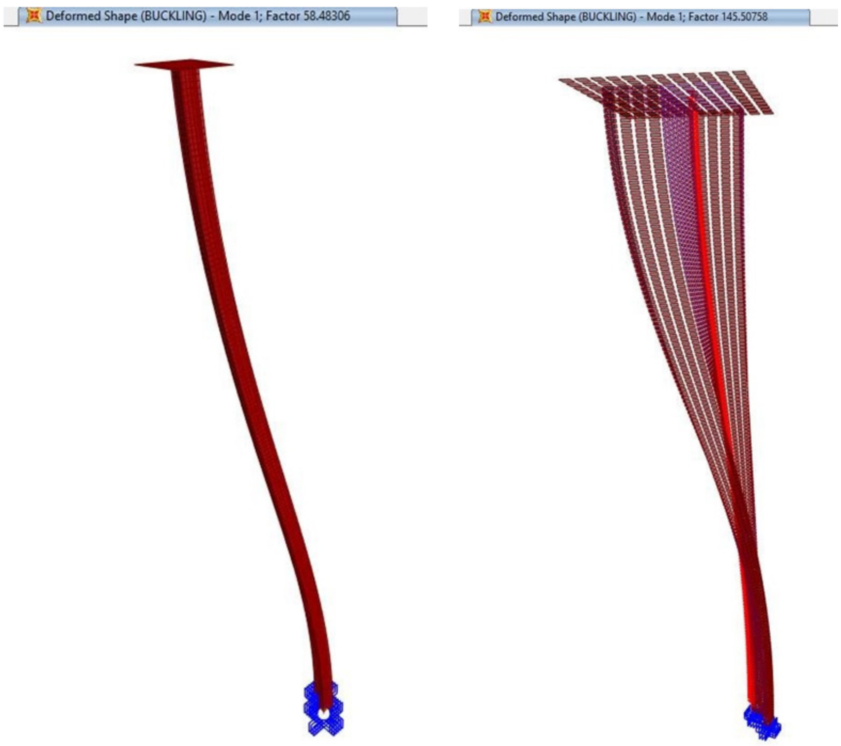

(a) (b)

Fig. 8 Deformed shape at the critical force for: (a) unrestrained, (b) laterally restrained column.

Table 2 Results of selected models.

	Critical forces F_{cr} [kN]			Design values N_{Ed} [kN] (EC3)
	Analytical analysis	Experimental test	Numerical analysis	
Unrestrained column	58.4	60	58.5	46.6
Restrained column	146.0	150	145.5	93.2
Relative increase	150%	150%	149%	100%

4. Design Critical Forces according to Eurocode 3

Simplified design of laterally restrained beams exists in EC3 [11], but it refers to purlins horizontally restrained by trapezoidal sheeting and loaded by the gravity or uplift load. It is strictly noted that method should not be used for application of axial forces. Thus, for laterally restrained columns subjected to axial force, critical forces should be determined from a complex analytical calculation using differential equations of stability, or by using numerical methods. According to EC3 [11, 15], imperfection factor is $\alpha = 0.34$ for buckling curve b.

For an unrestrained column, elastic critical force for the relevant buckling mode based on the gross cross-sectional properties is the value obtained by analytical analysis: $N_{cr} = F_{cr} = 58.4$ kN. For the yield strength $f_y = 306$ MPa, non-dimensional slenderness $\bar{\lambda} = 1.72$ and factor $\phi = 2.238$. Reduction factor for the relevant buckling mode is $\chi = 0.27 \leq 1$. Partial factor for resistance of members to instability assessed by member checks $\gamma_{M_1} = 1$. The design value of the compression force should be smaller or equal to the design buckling resistance of the compression member: $N_{Ed} \leq N_{b,Rd} = \frac{\chi A_S f_y}{\gamma_{M_1}} = 46.6$ kN.

For a laterally restrained column, elastic critical force for the relevant buckling mode based on the gross cross-sectional properties is obtained analytically: $N_{cr} = F_{cr} = 146.0$ kN. Additional data are: $\bar{\lambda} = 1.09$, $\phi = 1.245$, $\chi = 0.54 \leq 1$ and $N_{Ed} \leq N_{b,Rd} =$ 93.2 kN.

5. Presentation of the Results

Values of F_{cr} obtained by analytical (Section 2.5), experimental (Section 3.1) and numerical analysis (Section 3.2) of selected models are shown in Table 2. The design values N_{Ed} based on the critical forces obtained by EC3 (Section 4) are given as well.

6. Discussion and Conclusions

Analytical analysis for various lateral restraints (unrestrained column, column laterally restrained by a horizontal rigid connection, column laterally restrained by a vertical rigid connection and column laterally restrained by a horizontal rigid and rotational elastic connection) shows that buckling shape is different with and without lateral restraints, and critical forces are much larger in the latter case for buckling lengths considered (Table 1). The largest value of critical force is obtained for the column restrained by a horizontal rigid and rotational elastic connection (Section 2.4). Therefore, that case is selected for detailed analysis through experimental test and numerical calculation.

Critical forces obtained by analytical, numerical and experimental analysis of unrestrained and restrained column are close: the relative difference is less than 3% (Table 2). The relative increase in values of critical forces for a laterally restrained column compared to an unrestrained column is very large, regardless of the approach (about 150%). It is higher than for the design values N_{Ed} according to EC3 (100%). If we compare results with the buckling of the C-cross section models, the influence of lateral restraining on the Z-cross section columns is greater [8]. Relative increase of critical forces for the C-cross section is about 57% [8], while for the Z-cross section it is 150%.

Significant influence of lateral restraints on the stability of thin-walled Z-cross sections has been detected and further optimization of such structural elements is possible: critical forces are much larger if the model is laterally restrained. Also, relative increase of critical forces is higher, than for the design values obtained by to EC3.

References

[1] Schramm, U., and Pilkey, W. D. 1994. "Optimal Shape Design for Thin-Walled Beam Cross-Sections." *International Journal for Numerical Methods in Engineering* 37 (23): 4039-58. doi: 10.1002/nme.1620372307.

[2] Šimić, D. 2008. *The Theory of Thin-Walled Beams with Open Cross Section*. Manualia Universitatis Studiorum Zagrabiensis, Zagreb, Croatia.

[3] Dubina, D., Ungureanu, V., and Landolfo, R. 2012. *Design of Cold-Formed Steel Structures, Eurocode 3: Design of Steel Structures, Part 1-3: Design of Cold-formed Steel Structures, ECCS European Convention for Constructional Steelwork*. Brussels, Belgium.

[4] Zaras, J., Kowal-Michalska, K., and Rhodes, J. 2001. *Thin-Walled Structures—Advances and Developments*. Oxford, UK: Elsevier Science Ltd.

[5] Šimić, D. 2010. "The Impact of Lateral Restraint on the Stability of the Thin-Walled Z-Section Beam." Presented at 27th Symposium on Advances in Experimental Mechanics, Institute of Machines Design and Operation, Wroclaw.

[6] Ye, Z., Kettle, R. J., Li, L., and Schafer, B. W. 2002. "Buckling Behavior of Cold-Formed Zed-Purlins Partially Restrained by Steel Sheeting." *Thin-Walled Structures* 40 (10): 853-64. doi: 10.1016/S0263-8231(02)00029-0.

[7] Basaglia, C., Camotim, D., Gonçalves, R., and Graça, A. 2013. "GBT-Based Assessment of the Buckling Behaviour of Cold-Formed Steel Purlins Restrained by Sheeting." *Thin-Walled Structures* 72: 217-29. doi: 10.1016/j.tws.2013.06.005.

[8] Mališ, T., and Šimić Penava, D. 2017. "The Impact of Lateral Restraint on Structural Stability of Thin-Walled C-Cross Section Column Subjected to Axial Force." *Transactions of Famena* 41 (3): 13-28. doi: 10.21278/TOF.41302.

[9] Zienkiewicz, O. C., and Taylor, R. L. 2000. *The Finite Element Method*. 5th ed., Oxford, UK: Butterworth-Heinemann.

[10] Byars, E. F., and Snyder, R. D. 1964. *Engineering Mechanics of Deformable Bodies*. Highlighting edition. International Textbook Company.

[11] EN 1993-1-3: 2005 + AC 2009. *Eurocode 3: Design of Steel Structures—Part 1.3: General Rules—Supplementary Rules for Cold-Formed Members and Sheeting*. CEN: European Committee for Standardization. Brussels, Belgium.

[12] Higdon, A., Ohlsen, E. H., Stiles, W. B., Weese, J. A., and Riley, W. F. 1976. *Mechanics of Materials*. SI Version, 3rd ed., John Wiley & Sons.

[13] Paavola, J., and Salonen, S. 1992. "Flexural-Torsional Stability of Thin-Walled Columns." *Journal of Engineering Mechanics* 118 (12): 2384-400.

[14] Computers and Structures, Inc. 2011. *SAP2000 Analysis Reference Manual*. Berkeley, California, USA.

[15] EN 1993-1-1: 2005+AC 2009/A1:2014. *Eurocode 3: Design of Steel Structures—Part 1.1: General Rules and Rules for Buildings*. CEN: European Committee for Standardization. Brussels, Belgium.